COMPDYN 2015
5th ECCOMAS Thematic Conference on
Computational Methods in Structural Dynamics and Earthquake Engineering
M. Papadrakakis, V. Papadopoulos, V. Plevris (eds.)
Crete Island, Greece, 25–27 May 2015

ANALYSIS AND EXPERIMENT OF ISOLATED BRIDGES USING POLYNOMIAL ROCKING BEARINGS

T.Y. Lee[1], L.Y. Lu[2], J.H. Tzeng[3] and K.J. Chung[3]

[1] National Central University
Taoyuan County, Taiwan 32001, R.O.C.
tylee@ncu.edu.tw

[2] National Cheng Kung University
Tainan City, Taiwan 701, R.O.C.
lylu@mail.ncku.edu.tw

[3] National Central University
Taoyuan County, Taiwan 32001, R.O.C.
{993202017,100322016}@cc.ncu.edu.tw

Keywords: Variable-Curvature Seismic Isolator, Various-Frequency Seismic Isolator, Rocking Isolator, Near-Field Ground Motion, Shaking Table Test.

Abstract. *This paper is aimed to study the effectiveness of Polynomial Rocking Bearing (PRB), a various-frequency sliding isolator, in decreasing the seismic responses of isolated bridges. Although sliding isolators have been widely used to mitigate seismic hazard, it may be not effective in decreasing the seismic responses of isolated structures subjected to near-field ground motions. Near-field ground motions are of a pulse period which may be close to the natural periods of the isolated structures so as to lead the isolated structures to be resonant. Various-frequency sliding isolators could regulate the natural periods of the structures to avoid resonance under near-field ground motions. However, the key issue is how to choose the geometric shape and friction materials in design of various-frequency sliding isolators. This study adopts PRB to be the various-frequency sliding isolator whose rocking surface consisting of six-order polynomial. The restoring stiffness of the PRB possesses softening section as well as hardening section. The structural acceleration response can be decreased by decreasing the restoring stiffness in softening section while the structural displacement response can be decreased by increasing the restoring stiffness in hardening section. Since the PRB equivalent horizontal friction coefficient can be adjusted via the various geometric shapes, the friction material can be then arbitrarily chosen to increase the bearing reliability and durability. PSO-SA hybrid algorithm is used to find out the optimum parameters of the PRB in this study. A series of shaking table tests are conducted to demonstrate the effectiveness of the PRB in mitigating the dynamic responses of bridges under strong earthquakes. Numerical analysis is also performed to make comparison with the experiments. It shows the numerical results agree with the experimental results very well.*

1 INTRODUCTION

Seismic isolation is one of most effective technologies to protect structural systems and their interior equipment or facilities from earthquakes [1-2]. Different from conventional seismic resistance techniques, seismic isolation is to implement a soft layer under the protected structure, so that the seismic load transmitted onto the structure can be mitigated [3]. A seismic structure with a conventional isolation system is usually designed to be a long-period system with a fixed isolation frequency and damping ratio. Although these constant isolation parameters may be optimally designed for the given design earthquake, the existence of the long-period feature inevitably induces a low-frequency resonant-like response when the isolation system is subjected to a ground motion containing strong long-period components [4]. Many studies have found that an isolated structure with a conventional isolation system will exhibit excessive isolator displacement in near-field ground motions, whose waveforms usually possess a long-period pulse component [5]. Consequently, this will yield an unsuitable isolator design and increase the risk of superstructure pounding effect.

To avoid the low-frequency resonance problem that conventional isolators may encounter in long-period earthquakes, some researchers have suggested using isolators with variable mechanical properties, so the isolation systems may be adaptive to a wider range of earthquakes with different characteristics [6]. A new type of isolator called polynomial rocking bearings (PRB) is adopted for bridges in this study. The PRBs have variable isolation stiffness that can meet the desired design specifications. This study involves the experiment verification and numerical simulation of the seismic responses of an isolated bridge with PRBs. Moreover, the theory and formulas that describe the mechanical properties of a general PRB will be reviewed at the beginning of this paper. Then, based on the general formulas, the PRB used in the shaking table tests can be designed.

2 THEORY OF POLYNOMIAL ROCKING BEARINGS

2.1 Configuration of a PRB

Figure 1 illustrates a PRB installed between the deck and column in a bridge. The PRB has an articular (ball-and-socket) joint on the top and a concave rocking surface with a base plate on the lower part. The articular joint is mounted on the bottom of the deck with the sole plate while on the column with the base plate. In an earthquake, the rocking surface of the bearing will rock back-and-forth on the base plate, which provides an isolation layer to reduce the seismic induced forces transmitted onto the superstructure. The geometry of the rocking surface is usually axially symmetric about the vertical axis and must be concave. In order to provide variable isolation frequencies, the rocking surface may have a variable curvature that can be determined by the designer. However, the radius of the curvature has to be larger than the bearing height to maintain the stability during rocking. Moreover, there are three important design items for the rocking bearing including the bearing height, the radius of the spherical head and the sixth-order polynomial function defining the shape of the rocking surface. [6]

2.2 Mechanism of a PRB

The mechanical properties of an isolator are generally characterized by the relation between its horizontal shear and displacement. The formulas that describe this relation for a general PRB will be discussed below.

Figure 2 depicts the free-body diagram of a PRB where the friction on the spherical head is neglected because of insignificant effect. *xy* coordinate is fixed on the base plate while XY c-

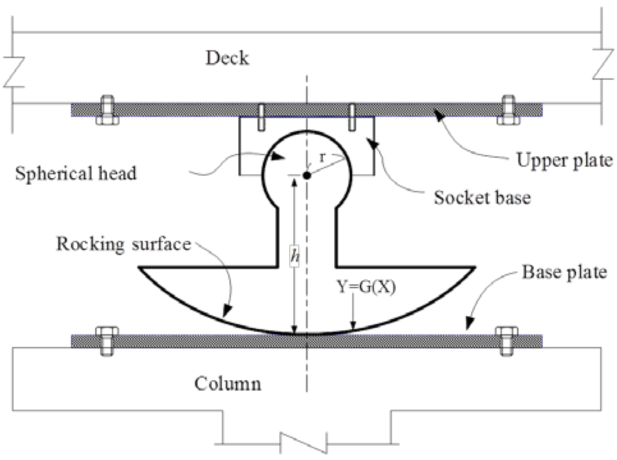

Figure 1: A PRB installed on a column

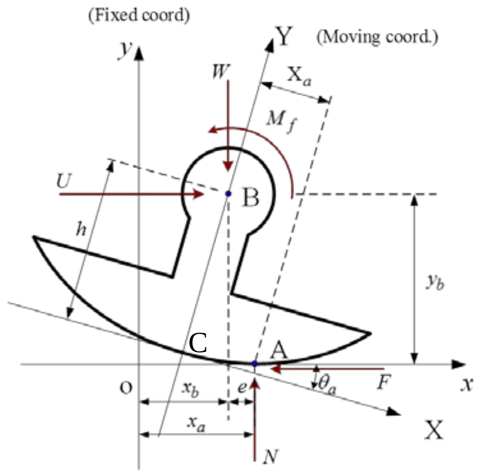

Figure 2: Free-body diagram of a PRB

-oordinate is moving with the rocking body. The rocking surface is defined by a sixth-order polynomial function, $\mathrm{Y} = \mathrm{G}(\mathrm{X})$. Assume that the rocking surface and the base plate intersect at point A. Therefore, the x-axis is always tangent to the rocking surface at the intersect A.

The vertical force *W* can be determined by the structural weights when neglecting vertical motion. The horizontal shear force *U* transmitted onto the isolated structure can be calculated by using the equilibrium equation of moments, i.e. $\sum M_A = 0$, as

$$U = u_r = \frac{We}{y_b} = \frac{W\left(x_a - x_b\right)}{y_b} \tag{1}$$

where u_r signifies the bearing restoring force; x_a is the *x* coordinate of the intersect A in the *xy* coordinate; x_b and y_b are the *x* and *y* coordinates of the point B, respectively. Since it is assumed that there is no relative sliding between the rocking surface and the base plate, x_a is equal to the arc length S_{ac} from point A to point C on the rocking surface. x_a, x_b, y_b and θ_a are determined by the following equations.

$$x_a = S_a = \int ds = \int_0^{\mathrm{X}_a} \left[1 + \left(G'(\mathrm{X}_a)\right)^2\right]^{1/2} d\mathrm{X} \tag{2}$$

$$x_b = \left(h - G(\mathrm{X}_a)\right)\sin\theta_a - \mathrm{X}_a\cos\theta_a + x_a \tag{3}$$

$$y_b = \left(h - G(\mathrm{X}_a)\right)\cos\theta_a + \mathrm{X}_a\sin\theta_a \tag{4}$$

$$\tan\theta_a = G'(\mathrm{X}_a) \quad ， \quad -\frac{\pi}{2} \le \theta_a \le \frac{\pi}{2} \tag{5}$$

where X_a represents the X coordinate of the point A.

Applying Eq. (5), Eqs. (3) and (4) can be rewritten as

$$x_b = \frac{\left(h - G(X_a)\right)G'(\mathrm{X}_a)}{\left[1 + \left(G'(\mathrm{X}_a)\right)^2\right]^{\frac{1}{2}}} - \frac{X_a}{\left[1 + \left(G'(\mathrm{X}_a)\right)^2\right]^{\frac{1}{2}}} + x_a \tag{6}$$

$$y_b = \frac{\left(h - G\left(X_a\right)\right)}{\left[1 + \left(G'\left(X_a\right)\right)^2\right]^{\frac{1}{2}}} + \frac{X_a G'\left(X_a\right)}{\left[1 + \left(G'\left(X_a\right)\right)^2\right]^{\frac{1}{2}}} \tag{7}$$

Substituting Eqs. (2), (6) and (7) in Eq. (1) yields

$$u_r = u_r\left(X_a\right) = \frac{W\left[-\left(h - G\left(X_a\right)\right)G'\left(X_a\right) + X_a\right]}{\left(h - G\left(X_a\right)\right) + X_a G'\left(X_a\right)} \tag{8}$$

Note that the restoring force u_r of a PRB is proportional to the vertical load *W*.

In order to improve the isolation performance for near-field earthquakes, the geometric function $Y = G\left(X\right)$ of the rocking surface may be defined by the following sixth-order polynomial function:

$$G\left(X\right) = c_1 X^6 + c_2 X^4 + c_3 X^2 \tag{9}$$

where c_1, c_2 and c_3 are three constant coefficients determined by designers. Next, applying Eq. (9) in Eq. (8) yields the fifth-order polynomial function for the isolator restoring force.

The stiffness k_r of a PRB can be defined as the rate of change of the restoring force u_r with respect to the isolator displacement x_b. However, since the restoring force u_r of a PRB is not an explicit function of x_b, the bearing stiffness k_r has to be computed indirectly by using the following equation

$$k_r = k_r\left(X_a\right) = \frac{du_r\left(X_a\right)}{dx_b\left(X_a\right)} = \frac{\left(\dfrac{du_r\left(X_a\right)}{dX_a}\right)}{\left(\dfrac{dx_b\left(X_a\right)}{dX_a}\right)} \tag{10}$$

Once the geometric function G(X) of the rocking surface is defined, the stiffness k_r can be calculated by Eq. (10). The restoring stiffness of the PRB can be divided into softening section and hardening section. The structural acceleration response can be decreased by decreasing the restoring stiffness in softening section while the structural displacement response can be decreased by increasing the restoring stiffness in hardening section. Since the PRB equivalent horizontal friction coefficient can be adjusted via the various geometric shapes, the friction material can be then arbitrarily chosen to increase the bearing reliability and durability.

3 NUMERICAL ANALYSIS

3.1 Simplified numerical model of bridges

Since bracing systems and shear connectors are always used in superstructures to interconnect all the steel girders and slabs as a solid deck, the deck of the typical isolated bridge may be assumed rigid in the longitudinal direction. Therefore, a column with an effective deck mass on the top can be taken apart as a unit for analysis as shown in Fig. 3

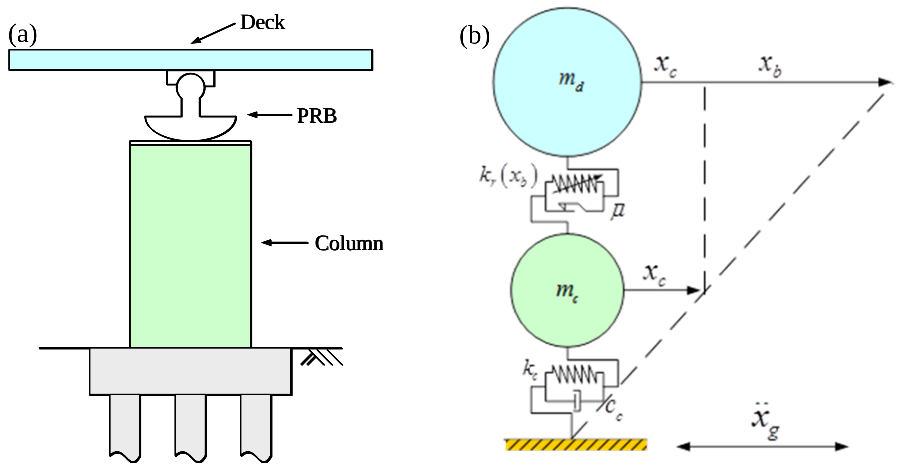

Figure 3: Analytical idealization (a) analytical unit (b) 2DOF system

3.2 Equations of Motion

The equations of motion for the isolated bridge with PRBs may be expressed as

$$\begin{bmatrix} m_d & m_d \\ 0 & m_c \end{bmatrix}\begin{bmatrix} \ddot{x}_b \\ \ddot{x}_c \end{bmatrix}+\begin{bmatrix} 0 & 0 \\ 0 & c_c \end{bmatrix}\begin{bmatrix} \dot{x}_b \\ \dot{x}_c \end{bmatrix}+\begin{bmatrix} 0 & 0 \\ 0 & k_c \end{bmatrix}\begin{bmatrix} x_b \\ x_c \end{bmatrix}=-\begin{bmatrix} m_d & 0 \\ 0 & m_c \end{bmatrix}\begin{bmatrix} 1 \\ 1 \end{bmatrix}\ddot{x}_g+\begin{bmatrix} u_r+u_f \\ -u_r-u_f \end{bmatrix} \tag{11}$$

Let $u(t)=u_r+u_f$ and rewrite Eq. (11) in vector form as:

$$\mathbf{M}\ddot{\mathbf{x}}(t)+\mathbf{C}\dot{\mathbf{x}}(t)+\mathbf{K}\mathbf{x}(t)=-\mathbf{M}_1\mathbf{L}_1\ddot{x}_g(t)+\mathbf{L}_2u(t) \tag{12}$$

where $\mathbf{x}$ is the displacement vector. $\ddot{x}_g$ is the ground acceleration. $\mathbf{M}$, $\mathbf{C}$, $\mathbf{K}$ and $\mathbf{M}_1$ are the mass matrix, damping matrix, stiffness matrix and distribution matrix of mass, respectively. $\mathbf{L_1}$ and $\mathbf{L_2}$ are the distribution matrices of seismic force and horizontal shearing force of PRBs, respectively.

The equations of motion, Eq. (12) can be rewritten in the state space as:

$$\dot{\mathbf{z}}(t)=\mathbf{A}\mathbf{z}(t)+\mathbf{E}\ddot{x}_g(t)+\mathbf{B}u(t) \tag{13}$$

The equations of motion, Eq. (13), in a continuous time system can be expressed in a discrete-time state-space form as

$$\mathbf{z}[k+1]=\mathbf{A}_d\mathbf{z}[k]+\mathbf{E}_0\ddot{x}_g[k]+\mathbf{E}_1\ddot{x}_g[k+1]+\mathbf{B}_0u[k]+\mathbf{B}_1u[k+1] \tag{14}$$

where a variable with [*k*] denotes the quantity is evaluated at the *k*th computational time step. All the matrices $\mathbf{A}_d$, $\mathbf{B}_0$, $\mathbf{B}_1$, $\mathbf{E}_0$ and $\mathbf{E}_1$ are constant coefficient matrices that are evaluated by using the following equations.

$$\mathbf{A}_d=e^{\mathbf{A}\Delta t}=\sum_{i=0}^{\infty}\frac{\Delta t}{i!}\mathbf{A}^i\ ,\ \mathbf{B}_0=\left(\sum_{i=0}^{\infty}\frac{(\Delta t)^{i+1}}{i!(i+2)}\mathbf{A}^i\right)\mathbf{B}\ ,\ \mathbf{B}_1=\left(\sum_{i=0}^{\infty}\frac{(\Delta t)^{i+1}}{(i+1)!}\mathbf{A}^i-\sum_{i=0}^{\infty}\frac{(\Delta t)^{i+1}}{i!(i+2)}\mathbf{A}^i\right)\mathbf{B}\ ,$$
$$\mathbf{E}_0=\left(\sum_{i=0}^{\infty}\frac{(\Delta t)^{i+1}}{i!(i+2)}\mathbf{A}^i\right)\mathbf{E}\ ,\ \mathbf{E}_1=\left(\sum_{i=0}^{\infty}\frac{(\Delta t)^{i+1}}{(i+1)!}\mathbf{A}^i-\sum_{i=0}^{\infty}\frac{(\Delta t)^{i+1}}{i!(i+2)}\mathbf{A}^i\right)\mathbf{E} \tag{15}$$

where Δt denotes the time interval of computation.

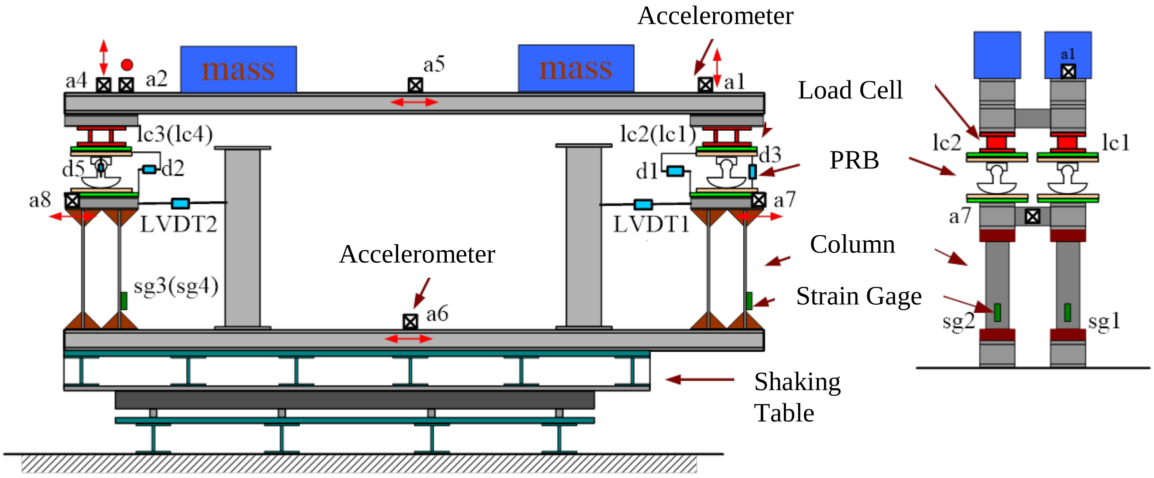

Figure 4: Test setup of a bridge with PRBs

4 EXPERIMENT OF A BRIDGE MODEL WITH PRBS

A series of shaking table tests are conducted to recognize the effectiveness of the PRBs in decreasing the induced seismic force for bridges. The experimental results are compared with the analysis results to verify the accuracy of the numerical model. Since we reused the PRBs studied by Lu et al. for buildings [7], the rocking surface may be not optimum for the bridge test model. However, after proving the feasibility of the PRBs, the optimum rocking surface will be searched by PSO-SA hybrid algorithm. Figure 4 illustrates the setup of the shaking table tests. Two ground motions recorded at El Centro, California 1940 and Imperial Valley 1979 are selected. El Centro records represent the far-field ground motions while Imperial Valley records represent the near-field ground motions.

4.1 Results of numerical analysis and experiment

The experimental and analytical results under El Centro and Imperial Valley ground motions are compared in Figs. 5 and 6. Figures 5(a), 5(b) and 5(c) show the time histories of the deck displacement, bearing displacement and column displacement, respectively, under El Centro ground motion with PGA of 307 gal. Figure 5(d) shows the hysteresis loop of the PRB under El Centro ground motion. Figure 6 shows the comparison under Imperial Valley ground motion with PGA of 350 gal. Observed from the results, the numerical model is able to satisfactorily simulate the dynamic behavior of the isolated bridge with PRBs. Besides, the effectiveness of PRB isolation can be estimated in the experiment. Table 1 shows the comparison between the isolated bridge with PRBs and non-isolated bridge. Obviously, the peak column displacement largely decreases in the isolated bridge with PRBs as compared to the non-isolated bridge under both far-field and near-field ground motions.

Table 1: Comparison between the isolated bridge with PRBs and non-isolated bridge

Ground Motion	PGA (g)	Peak Column Displacement with PRB (cm)	Peak Column Displacement w/o PRB (cm)	Percentage of reduction (%)
El Centro	0.307	1.46	6.33	76.9
Imperial Valley	0.350	1.58	4.62	65.8

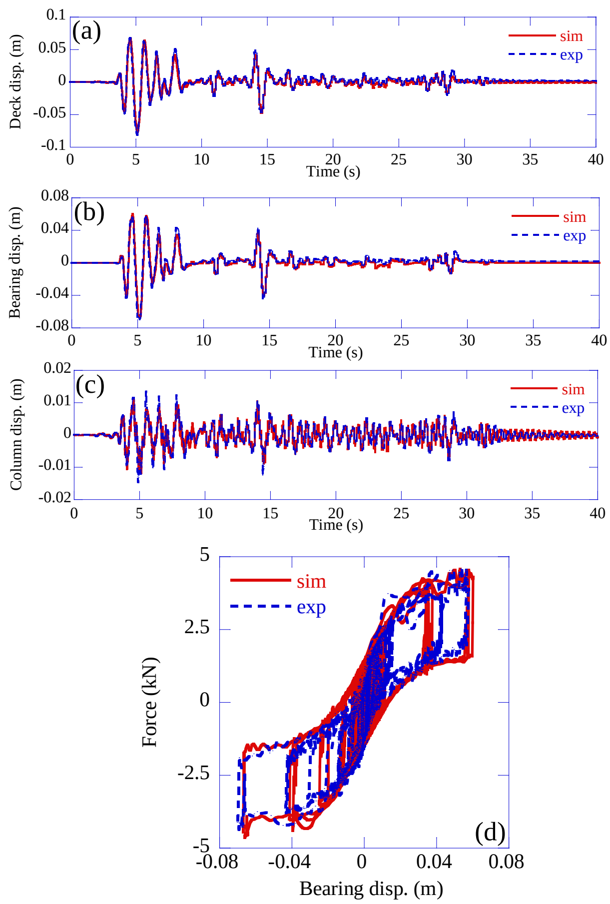

Figure 5: (a) deck displacement (b) bearing displacement (c) column displacement (d) hysteresis loop of PRBs under El Centro ground motion

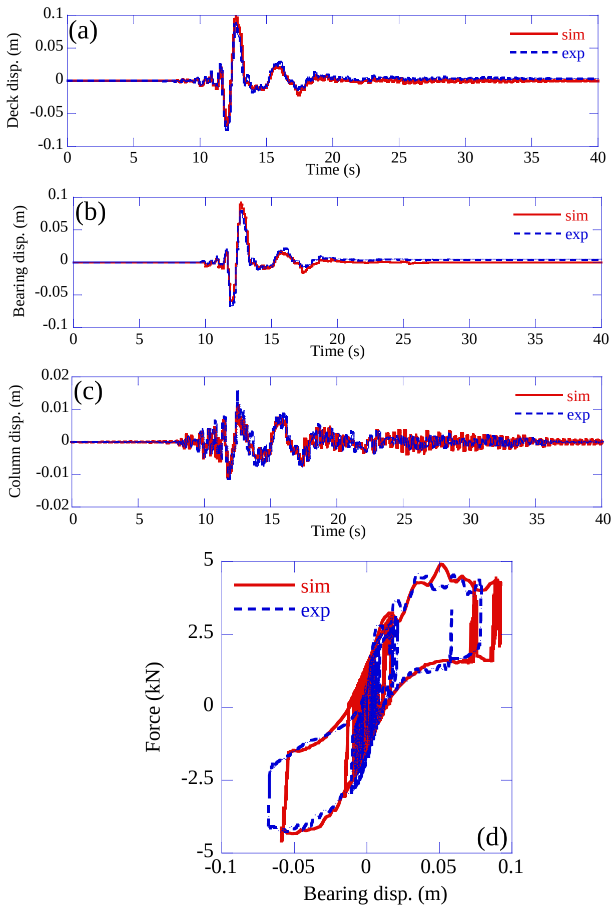

Figure 6: (a) deck displacement (b) bearing displacement (c) column displacement (d) hysteresis loop of PRBs under Imperial Valley ground motion

5 DESIGN OF PRBS

The effect of PRBs on the seismic behavior is influenced by the six-order polynomial of rocking surface, bearing height and equivalent friction coefficient. It is extremely tedious and time-consuming to perform a parametric study for exploring the optimum parameters. Optimization techniques are expected to provide a smart solution to such an optimization problem. In this study, PSO-SA hybrid searching algorithm is adopted to explore the optimum design parameters of PRBs. [8]

In order to reveal the efficiency of the PRBs, a friction pendulum system (FPS), a traditional sliding bearing, is also investigated in this study for comparison. The design parameters of both the PRBs and FPSs are determined by using PSO-SA hybrid searching algorithm. Figures 7 and 8 compare the dynamic responses of the isolated bridges with PRBs and FPSs under El Centro records and Imperial Valley records, respectively. Table 2 shows the peak responses of bridges under two records. The simulation results indicate that the column and deck displacements of the isolated bridge with PRBs are further decreased as compared with FPSs.

Table 2: Peak responses of isolated bridges

Ground Motion	Peak Bearing Displacement (cm)		Peak Column Displacement (cm)		Peak Deck Displacement (cm)	
	PRB	FPS	PRB	FPS	PRB	FPS
El Centro	4.23	4.04	1.91	2.04	4.14	4.24
Imperial Valley	6.29	9.13	2.52	2.59	8.49	10.90

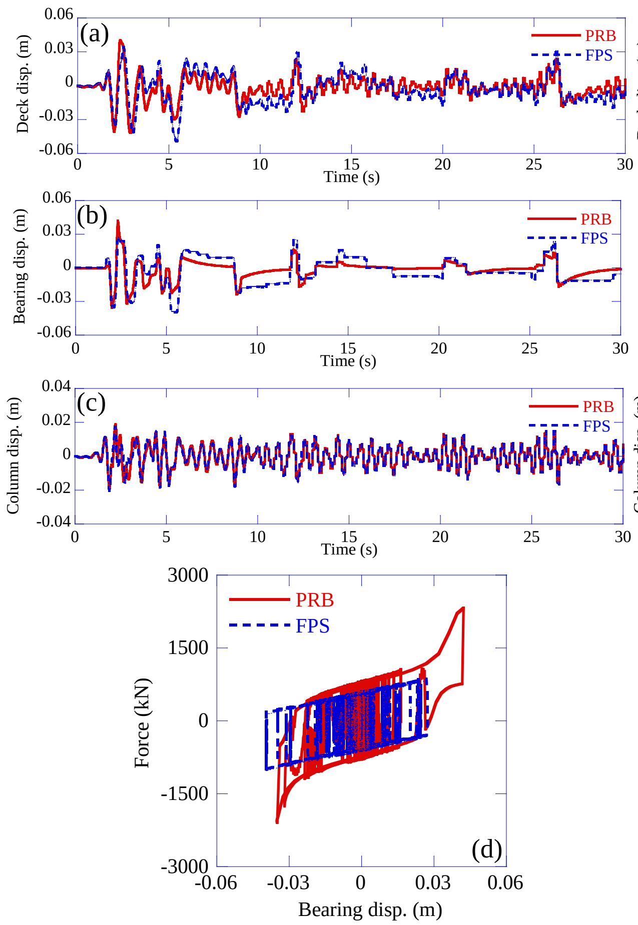

Figure 7: (a) deck displacement (b) bearing displacement (c) column displacement (d) hysteresis loop of PRBs and FPSs under El Centro records

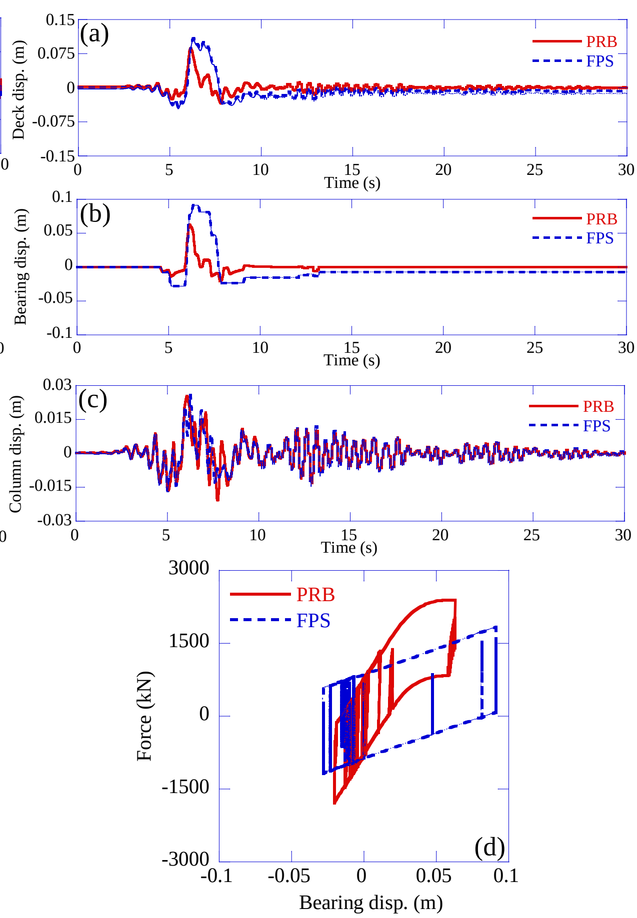

Figure 8: (a) deck displacement (b) bearing displacement (c) column displacement (d) hysteresis loop of PRBs and FPSs under Imperial Valley records

6 CONCLUSIONS

- A new type of isolator called polynomial rocking bearing (PRB) is applied to bridges in this study. Through shaking table tests, the results reveal the feasibility and effectiveness of PRBs in mitigating the dynamic responses of bridges under both near-field and far-field ground motions as compared to the non-isolated bridges. Also, the numerical model is verified to be accurate in simulation of the isolated bridge with PRBs.

- Since the restoring stiffness of the PRB can be divided into softening section and hardening section, the structural acceleration response can be decreased in softening section while the structural displacement response can be decreased in hardening section. As compared to the traditional FPS, the column and deck displacements of the isolated bridge with PRBs can be further improved under both near-field and far-field ground motions.
- The effect of PRBs on the seismic behavior is influenced by the six-order polynomial of rocking surface, bearing height and equivalent friction coefficient. Such design parameters can be determined by using PSO-SA hybrid searching algorithm. From the results of numerical simulations, it is verified that the PRBs can reach the optimum performance in mitigating the seismic responses of bridges.

REFERENCES

[1] C. Christopoulos, A. Filiatrault, Principles of passive supplemental damping and seismic isolation. *IUSS Press*. Pavia, 2006.

[2] F. Naeim, J.M. Kelly, Design of seismic isolated structures: from theory to practice. *John Wiley & Sons*, 1999.

[3] Y.B. Yang, L.Y. Lu, J.D. Yau, C.W. de Silva (Ed.), Structure and equipment isolation, vibration and shock handbook. *CRC Press,* Taylor & Francis Group, 2005.

[4] W.L. He, A.K. Agrawal, Analytical model of ground motion pulses for the design and assessment of seismic protective systems. *J Struct Eng*, **134**, 1177-1188, 2008.

[5] L.Y. Lu, G.L. Lin, M.H. Shih, An experimental study on generalized Maxwell model for nonlinear viscous dampers used in seismic isolation. *Eng Struct*, **34**, 111-123, 2012.

[6] L.Y. Lu, C.C. Hsu, Experimental study of variable-frequency rocking bearings for near-fault seismic isolation. *Eng Struct*, **46**, 116-129, 2013.

[7] L.Y. Lu, T.Y. Lee, I.L. Yeh, H. Chang, Rocking bearings with variable frequency for near-fault seismic isolation (in Chinese). *Journal of the Chinese Institute of Civil and Hydraulic Engineering*, **22**, 283-298, 2010.

[8] T.Y. Lee, P.C. Chen, D.S. Juang, Sliding mode control on isolated bridge with columns of irregular heights using pole assignment and PSO-SA hybrid algorithm. *International Journal of Structural Stability and Dynamics*, **12**, 1250014 (26pages), 2012.